Chapter 10

The First Single-Photon Sources

Alain Aspect and Philippe Grangier
Laboratoire Charles Fabry, Institut d'Optique, CNRS, Univ Paris-Sud, 2 Avenue Augustin Fresnel, 91127 Palaiseau, France

Chapter Outline

Single-Photon Generation and Detection, Volume 45. http://dx.doi.org/10.1016/B978-0-12-387695-9.00010-X
© 2013 Elsevier Inc. All rights reserved.

10.1 INTRODUCTION

This chapter shows how the concept of single-photon sources has emerged, starting in the early 1980s. It presents the quantum optics approach to "single-photon states" and "single-photon wavepackets." The quantum behavior of such states—a single photon yields one photodetection only—is contrasted with the behavior of attenuated classical lights, which always yield some possibility of a joint detection on both sides of a beam splitter. We describe the single-photon source that we developed in the early 1980s at Institut d'Optique, as well as the quantitative criterion ("*anticorrelation*") that we introduced and used in a real experiment to show that it was indeed a single-photon source. We contrast these results with the ones that we obtained with a source of classical light pulses produced by a strongly attenuated light-emitting diode driven by nanosecond electric pulses. Such light pulses do not pass the anticorrelation test, and are definitely not single-photon pulses. We also describe the interference experiment we carried out with our single-photon source, which illustrates the notion of wave-particle duality. We conclude with a brief overview of further developments in sources of single photons, heralded or on-demand, as well as in wave-particle duality experiments, in particular Wheeler's delayed-choice experiments.

The rapidly developing field of quantum information [1] makes wide use of two types of sources of quantum light: sources of single photons on the one hand, and sources of pairs of entangled photons on the other hand. One might think that single-photon sources were developed first, but it turns out that the history is just the opposite: in the optical domain, sources of pairs of entangled photons were invented first, and only later came single-photon sources. This happened first with the source of entangled photons of Clauser and Freedman [2], about which a property related to the behavior of single photons was demonstrated two years later [3]. In the same vein, it took five years for the more efficient source of pairs of entangled photons of Aspect *et al.* [4], to be explicitly used and characterized, by Grangier and Aspect, as the first source of single photons [5]. Similarly, the first source of pairs of correlated photons produced by parametric down-conversion [6,7] preceded the use of that source to produce single photons by Mandel *et al.* [8]. Actually, all these single-photon sources were what is called, in modern quantum optics language, "heralded single-photon sources," i.e., single-photon wavepackets whose leading-edge time—or peak time in the case of a bell-shaped pulse—is known by the observation of the other photon of a pair [9]. This is why their development obviously demanded the existence of a source of pairs of photons correlated in time. It took almost another two decades until the first source of single photons "on-demand" appeared [10], i.e., a source of single-photon wavepackets whose leading-edge time can be chosen at will.

Although the question of single photons had been raised at the beginning of the 20th century in the context of single-photon interference (see Section 10.2.1), the question remained confused until the early 1980s, when we

realized that none of the so-called "single-photon interference experiments" had been carried out with "one-photon states of light." Indeed, all these experiments had been performed with feeble-light beams issued from standard sources (such as discharge lamps), and it was clear from the formalism of quantum optics, that however weak, such lights could be described by quasi-classical states [11,12]. Therefore, their properties could be understood by the semi-classical model of matter-light interaction, in which light is described as a classical electromagnetic wave, and the notion of a single photon has no meaning. Inspired by the experiment of Clauser [3], and by the celebrated antibunching experiment of Kimble-Dagenais-Mandel [13], we found a simple quantitative criterion to test a characteristic property of a single photon, *anticorrelation*: when sent to a beam splitter, a single photon (i.e., a one-photon state of the quantized electromagnetic field) can be detected either on one side or on the other side of the beamsplitter, but never jointly on both sides. This is in contrast to the behavior of light that can be described by a classical wave, which is split on the beam splitter and always yields some possibility of a joint detection on both sides of the beam splitter. We thus had a criterion that could be used for a test of the single-photon character of the light emitted by a source, not only theoretically, but also experimentally.

Section 10.2 of this chapter is devoted to a detailed theoretical presentation, in the formalism of quantum optics (kept as simple as possible), of the difference between light emitted by true sources of single photons, and light emitted by any other source, as feeble as it may be. The main conclusion is that light from other sources, no matter how weak, does not have the same characteristic property as single photons. Even in the case of a strongly attenuated discharge lamp where it is tempting to describe the light as made of single-photon wavepackets separated from each other, it does not pass the single-photon test since we miss the information about the time at which each individual single-photon wavepacket is emitted.

In Section 10.3, we give some details about the single-photon source that we developed in the early 1980s, and about the precise quantitative anticorrelation criterion that we introduced and used in an experiment to show that it was indeed a single-photon source. We contrast these results with the ones that we obtained with a source of classical light pulses produced by a light-emitting diode (LED) driven by nanosecond electric pulses, and attenuated to an average level of 10^{-2} photons per pulse. Such light pulses do not pass the single-photon test, and are definitely not single-photon pulses.

In Section 10.4, we give some details about the interference experiment we carried out with our single-photon source. Combined with the experiment of Section 10.3 that uses the same source, it yields a striking demonstration of the so-called "wave-particle duality," one of the two "great mysteries" of quantum mechanics according to Feynman [14], and it can be used for an introductory course in quantum optics [15–17] (see also [18]).

Section 10.5 sketches further developments of modern sources of single photons, either heralded or on-demand, without many details, since these details can be found in other chapters of this book. We also mention further experiments on wave-particle duality, and in particular on Wheeler's delayed-choice experiment [19], which has been performed not only in its original form [20], but also in a more refined version [21,22].

Remark on Vocabulary

In this chapter, we use the wordings "single photon," "single-photon wavepacket," "single-photon pulse" on the one hand, and "one-photon wavepacket" on the other hand. Although these wordings are almost equivalent, we tend to use "single photon" as it would be used generically in the common language, or in the language of a general physicist, while we give to "one-photon wavepacket" a more technical meaning, i.e., a state of the light that is an eigenstate of the quantum observable "Number of Photons" of the formalism of Quantum Optics (Section 10.2.2).

10.2 FEEBLE LIGHT VS. SINGLE PHOTON

10.2.1 In Search of Feeble Light's Wave-Like Properties: A Short Historical Review

Almost as soon as Einstein introduced the notion of a quanta of light [23], i.e., a relativistic particle [24] of energy $\hbar\omega$ and momentum $\hbar\omega/c$, the question of the wave-like behavior of the corresponding particle became a major concern among physicists, including Einstein himself [25]. The first attempt to investigate the question experimentally [26] consisted of registering on a photographic plate the diffraction pattern of a needle illuminated with extremely attenuated light, so that the energy flux expressed in the number of photons per second would correspond to an average distance between the photons much larger than the size of the apparatus. This pioneering experiment was followed by a long series of diffraction [27] and interference [28–33] experiments with light emitted by strongly attenuated ordinary light sources, mostly discharge lamps, so that the average rate of photons entering the interferometric device, estimated as the power divided by the energy of a photon, ranged between 10^2 and 10^7 s^{-1}. Even at the largest of these rates, the average distance between photons was more than 10 m, much larger than the size of the interferometric device used in the corresponding experiment. It was thus concluded that "there was only one photon at a time in the interferometer," and the observation of fringes was then considered a demonstration that "a photon interferes with itself." Actually, one experiment [30] failed to observe the interference pattern expected for a wave, but it was soon repeated by other scientists who found the expected interference pattern [32]. There is thus little doubt that diffraction or

interference phenomena can be observed even in conditions of very weak light intensity.

In the 1970s, the general wisdom was then that "single-photon wave-like behavior" had been experimentally demonstrated. However, revisiting that question in the early 1980s, we realized that, according to the formalism of modern quantum optics as developed by Glauber [12,34,35], none of the experiments cited above could be considered a demonstration of single particle interference, because in none of these experiments the light used could be considered as a single-photon wavepacket. This led us to perform the experiments of [5], presented in Sections 10.3 and 10.4. In the rest of this section, we use the formalism of quantum optics to highlight the difference between single-photon wavepackets and all the types of light used in the experiments above.

10.2.2 Quantum Optics in a Nutshell

We describe light in the standard formalism of quantum optics [17,36,37], in the Heisenberg representation. A particular light field is represented by a state vector independent of time $|\Psi\rangle$. When fluctuations must be accounted for, taking the statistical average will be sufficient, so we will not resort to the density matrix formalism nor to the notion of mixed states. The field observables depend on time (and position). The electric-field operator is decomposed into two adjoint operators, $\hat{\mathbf{E}}^{(-)}(\mathbf{r},t)$ and $\hat{\mathbf{E}}^{(+)}(\mathbf{r},t)$, corresponding respectively to positive and negative frequencies. These operators can be expanded on any set of modes of the electromagnetic field. A frequent choice is polarized homogeneous traveling waves, and the electric-field operator expansion then reads

$$\hat{\mathbf{E}}^{(+)}(\mathbf{r},t) = \mathrm{i}\sum_{\ell} \mathcal{E}_{\ell}^{(1)} \overrightarrow{\varepsilon_\ell}\, \hat{a}_\ell \exp[\mathrm{i}(\mathbf{k}_\ell \cdot \mathbf{r} - \omega_\ell t)], \tag{10.1}$$

$$\hat{\mathbf{E}}^{(-)}(\mathbf{r},t) = [\hat{E}^{(+)}(\mathbf{r},t)]^{\dagger}. \tag{10.2}$$

The mode ℓ is characterized by a wave-vector $\mathbf{k}_\ell$, an angular frequency $\omega_\ell = c|\mathbf{k}_\ell|$, and a polarization $\overrightarrow{\varepsilon_\ell}$ orthogonal to $\mathbf{k}_\ell$. The quantity

$$\mathcal{E}_{\ell}^{(1)} = \sqrt{\frac{\hbar\omega_\ell}{2\varepsilon_0 L^3}} \tag{10.3}$$

is the "one-photon amplitude." It depends on the volume of quantization L^3, which is usually arbitrary, so that L should not appear explicitly in the final results of the calculations.

The adjoint operators $\hat{a}_\ell$, and $\hat{a}_\ell^{\dagger}$ are the destruction and creation operators for photons of the mode ℓ. They obey the fundamental commutation relations

$$[\hat{a}_\ell, \hat{a}_{\ell'}^{\dagger}] = \delta_{\ell\ell'} \tag{10.4}$$

with $\delta_{\ell\ell'}$, the Kronecker symbol. They allow one to build a complete basis $\{|n_\ell\rangle;\, n_\ell = 0,1\ldots\}$ of the state space associated with the mode ℓ:

$$\hat{a}_\ell^\dagger |n_\ell\rangle = \sqrt{n_\ell + 1}|n_\ell + 1\rangle, \tag{10.5}$$

$$\hat{a}_\ell |n_\ell\rangle = \sqrt{n_\ell}|n_\ell - 1\rangle, \tag{10.6}$$

$$a_\ell |0_\ell\rangle = 0. \tag{10.7}$$

States $|n_\ell\rangle$, the so-called *number states*, are eigenstates of the operator "number of photons in the mode ℓ ":

$$\hat{N}_\ell = \hat{a}_\ell^\dagger \hat{a}_\ell, \tag{10.8}$$

the corresponding eigenvalue being precisely the number of photons n_ℓ:

$$\hat{N}_\ell |n_\ell\rangle = n_\ell |n_\ell\rangle. \tag{10.9}$$

One also defines the operator "total number of photons"

$$\hat{N} = \sum_\ell \hat{N}_\ell, \tag{10.10}$$

which can be measured with a wide-band photodetector operating in the photon-counting regime ("click detector").

There is no position operator for the photon, so one cannot define a density of probability of presence, as in the quantum mechanical description of a single massive particle. However, there is a very useful quantity that allows one to link theory to experiments with a click detector: the probability of a photodetection per unit of surface and time at the point $\mathbf{r}$ and time t. For a field in the state $|\Psi\rangle$, that quantity (also called the rate of single photodetections) is

$$w^{(1)}(\mathbf{r},t) = s\langle\Psi|\hat{\mathbf{E}}^{(-)}(\mathbf{r},t)\hat{\mathbf{E}}^{(+)}(\mathbf{r},t)|\Psi\rangle, \tag{10.11}$$

where s is the sensitivity of the detector. A most important quantity for modern quantum optics relates to the rate of double photodetections at $(\mathbf{r},t)$ and $(\mathbf{r}',t')$, which is defined by

$$d^2\mathcal{P} = w^{(2)}(\mathbf{r},t;\mathbf{r}',t')\mathrm{d}t\,\mathrm{d}t', \tag{10.12}$$

where $d^2\mathcal{P}$ is the probability of a double photodetection per unit surface around $\mathbf{r}$ during the time interval $[t,t+\mathrm{d}t]$ and per unit surface around $\mathbf{r}'$ during $[t',t'+\mathrm{d}t']$, with

$$w^{(2)}(\mathbf{r},t;\mathbf{r}',t') = s^2\langle\Psi|\hat{\mathbf{E}}^{(-)}(\mathbf{r},t)\hat{\mathbf{E}}^{(-)}(\mathbf{r}',t')\hat{\mathbf{E}}^{(+)}(\mathbf{r}',t')\hat{\mathbf{E}}^{(+)}(\mathbf{r},t)|\Psi\rangle. \tag{10.13}$$

The formalism above, and in particular the rates of single or double detections, will allow us to compare the properties of one-photon pulses with other types of lights: attenuated classical light pulses, attenuated laser beams, and light emitted from discharge lamps, attenuated or not.

Remark. Formulae (10.11) and (10.13) look similar to the semi-classical expressions for a classical electromagnetic field

$$\mathbf{E}_{\mathrm{cl}}(\mathbf{r},t) = \mathbf{E}^{(-)}(\mathbf{r},t) + \mathbf{E}^{(+)}(\mathbf{r},t), \tag{10.14}$$

where $\mathbf{E}^{(+)}(\mathbf{r},t)$ is the complex amplitude of the field, and $\mathbf{E}^{(-)}(\mathbf{r},t)$ its complex conjugate. The rates of single and double photodetections are indeed, in the semi-classical point of view,

$$w^{(1)}(\mathbf{r},t) = s\mathbf{E}^{(-)}(\mathbf{r},t)\cdot\mathbf{E}^{(+)}(\mathbf{r},t) = \eta|\mathbf{E}^{(+)}(\mathbf{r},t)|^2 \tag{10.15}$$

and

$$w^{(2)}(\mathbf{r},t;\mathbf{r}',t') = s^2|\mathbf{E}^{(+)}(\mathbf{r},t)|^2|\mathbf{E}^{(+)}(\mathbf{r}',t')|^2. \tag{10.16}$$

The semi-classical and quantum expressions are, however, dramatically different both technically and conceptually. In the quantum formalism, the non-commutation of $\hat{\mathbf{E}}^{(-)}$ and $\hat{\mathbf{E}}^{(+)}$ entails the fact that the probability of a double detection is null for a single photon, as can be seen in Section 10.2.5. Such a statement does not hold in the semi-classical point of view. More generally, in the fully quantum point of view, observation of a photoelectron at time t and location $\mathbf{r}$ is associated with a photon being detected at $(\mathbf{r},t)$. If the photodetector is perfect, each detected photoelectron is therefore associated with a photon. In other words, the statistical distribution of the photoelectrons reflects the statistical distribution of the photons in the beam. This is in contrast to the semi-classical point of view, where there is no photon, and the discrete and probabilistic character of the photodetection signals stems from the discretization of the electric charge, or equivalently from the discontinuous and probabilistic character of the photodetection process itself, while the classical light intensity $|\mathbf{E}^{(+)}(\mathbf{r},t)|^2$ is a continuous quantity.

10.2.3 One-Photon Wavepacket

Any light state of the form

$$|1\rangle = \sum_{\ell} c_\ell |n_\ell = 1\rangle \tag{10.17}$$

is an eigenstate of $\hat{N}$ (see Eq. (10.10)) corresponding to the eigenvalue 1. It is a one-photon state. As a model of such a state in a collimated beam, we consider a one-photon state consisting of modes all propagating along the same direction defined by the unit vector $\mathbf{u}$, i.e.,

$$\mathbf{k}_\ell = \mathbf{u}\frac{\omega_\ell}{c}. \tag{10.18}$$

Equation (10.11) then gives the rate of photodetections:

$$w^{(1)}(\mathbf{r},t) = \eta \left\| \sum_\ell \overrightarrow{\varepsilon_\ell}\, \mathcal{E}_\ell^{(1)} c_\ell \exp\left[-\mathrm{i}\omega_\ell \left(t - \frac{\mathbf{r}\cdot\mathbf{u}}{c}\right)\right] |0\rangle \right\|^2$$
$$= \eta \left| \sum_\ell \overrightarrow{\varepsilon_\ell}\, \mathcal{E}_\ell^{(1)} c_\ell \exp\left[-\mathrm{i}\omega_\ell \left(t - \frac{\mathbf{r}\cdot\mathbf{u}}{c}\right)\right] \right|^2, \qquad (10.19)$$

which suggests a propagation along $\mathbf{u}$ at velocity c.

To simplify formulae, we write most often such quantities at $\mathbf{r} = 0$. The expression at $\mathbf{r}$ is readily obtained replacing t by $t - \mathbf{r}\cdot\mathbf{u}/c$.

To be more specific, let us consider the case of a Lorentzian distribution for $|c_\ell|^2$, which happens to describe light emitted by two-level-like single emitters, such as single atoms. More precisely, we take the form

$$c_\ell(t_j) = \frac{K_1}{\omega_\ell - \omega_0 + \mathrm{i}\Gamma/2}, \qquad (10.20)$$

with

$$K_1 = |K_1| \exp\left(\mathrm{i}\omega_\ell t_j\right), \qquad (10.21)$$

such that the state vector is normalized. For simplification, we take all modes to have the same polarization,

$$\overrightarrow{\varepsilon_\ell} = \overrightarrow{\varepsilon}. \qquad (10.22)$$

For L large enough, the sum in (10.19) can be transformed into an integral using the density of modes $\rho(\omega)$. If Γ is small compared to ω_0, the quantities $\mathcal{E}_\ell^{(1)}, \rho(\omega)$, and $|K_1|$ can be considered constant in the integral, with their values at ω_0. The remaining integral can be calculated by integration in the complex plane, yielding:

$$E_{t_j}^{(1)}(t) = \sum_\ell \mathcal{E}_\ell^{(1)} c_\ell \mathrm{e}^{-\mathrm{i}\omega_\ell t} = \rho(\omega_0)\mathcal{E}_{\omega_0}^{(1)} |K_1| \int \mathrm{d}\omega \frac{\exp[-\mathrm{i}\omega(t-t_j)]}{\omega - \omega_0 + \mathrm{i}\Gamma/2}$$
$$= -2\mathrm{i}\pi\rho(\omega_0)\mathcal{E}_{\omega_0}^{(1)} K_1 \mathrm{H}(\tau) \exp\left[\left(-\frac{\Gamma}{2} - \mathrm{i}\omega_0\right)(t-t_j)\right]$$
$$= E_0 \mathrm{H}(t-t_j) \exp\left[\left(-\frac{\Gamma}{2} - \mathrm{i}\omega_0\right)(t-t_j)\right], \qquad (10.23)$$

where $\mathrm{H}(t)$ is the Heaviside step function. The rate of photodetection at $\mathbf{r} = 0$ is then

$$w^{(1)}(0,t) = \eta |E_{t_j}^{(1)}(t)|^2 = \eta |E_0|^2 \mathrm{H}(t-t_j) \exp[-\Gamma(t-t_j)]. \qquad (10.24)$$

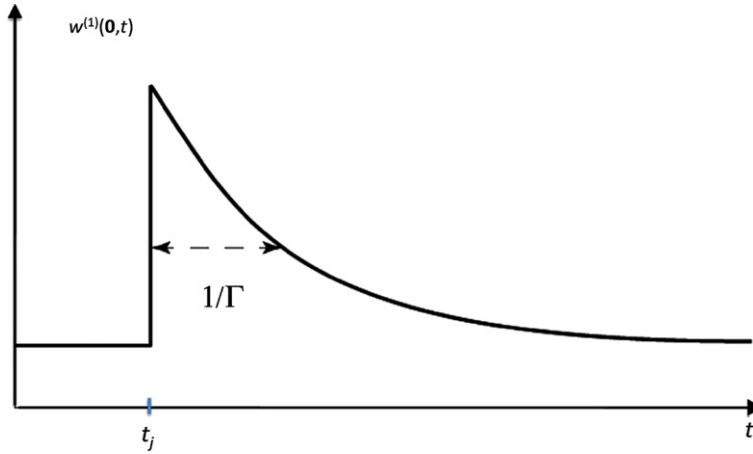

FIGURE 10.1 Average rate of photodetection at point at $\mathbf{r} = 0$ as a function of time, as given by Eq. (10.24) for a one-photon wavepacket with a leading edge at t_j. The rate of photodetection at point at $\mathbf{r}$ would be similar, with t_j replaced by $t_j + \mathbf{r}\cdot\mathbf{u}/c$.

Normalization of the state (10.17) with the coefficients c_ℓ given by (10.20) yields the condition

$$1 = \sum_\ell |c_\ell|^2 = \int \mathrm{d}\omega\, \rho(\omega) \frac{|K_1|^2}{(\omega - \omega_0)^2 + \Gamma^2/4}$$
$$= \frac{2\pi}{\Gamma} \rho(\omega_0) |K_1|^2. \tag{10.25}$$

Hence

$$E_0 = -\mathrm{i}\mathcal{E}^{(1)}_{\omega_0} [2\pi\rho(\omega_0)\Gamma]^{1/2}. \tag{10.26}$$

The rate of photodetection (10.24) at point $\mathbf{r} = 0$ is represented as a function of time in Fig. 10.1. It clearly suggests a wavepacket with a leading-edge at $t = t_j$, exponentially damped with a time constant Γ^{-1}. The result (10.24), however, must be understood in a statistical sense. One prepares a field in the form defined by Eqs. 10.17–10.20 at time $t = 0$, and one looks for photodetection by a detector at position $\mathbf{r}$. When the photodetection happens, its time is recorded. The experiment is repeated a great number of times, and the histogram of the results looks as shown in Fig. 10.1.

The one-photon state (10.17), of the form defined by (10.20), with (10.25), can be called a "one-photon wavepacket" with a leading-edge at t_j. We thus introduce the notation

$$|1(t_j)\rangle = \sum_\ell \frac{|K_1| \exp\left(\mathrm{i}\omega_\ell t_j\right)}{\omega_\ell - \omega_0 + \mathrm{i}\Gamma/2} |1_\ell\rangle. \tag{10.27}$$

The ensemble of these states, for all possible leading-edge times t_j, has properties that allow us to use them as a basis for all single-photon states. To show this, we establish a closure relation. We first introduce a *constant* density of states ρ_j, which has the dimension of an inverse time. We can then write

$$\sum_j |1(t_j)\rangle\langle 1(t_j)| = \rho_j \int \mathrm{d}t_j |1(t_j)\rangle\langle 1(t_j)|. \tag{10.28}$$

Let us now express $|1(t_j)\rangle$ replacing $\sum_\ell$ by an integral in (10.17), with (10.20) and the density of states $\rho(\omega_\ell)$. We obtain

$$\sum_j |1(t_j)\rangle\langle 1(t_j)| = \rho_j \int \mathrm{d}t_j \iint \mathrm{d}\omega_\ell \, \mathrm{d}\omega_{\ell'} \, \rho(\omega_\ell)\rho(\omega_{\ell'}) \times \frac{|K_1|^2 \exp \mathrm{i}(\omega_\ell - \omega_{\ell'})t_j}{\left(\omega_\ell - \omega_0 + \mathrm{i}\frac{\Gamma}{2}\right)\left(\omega_{\ell'} - \omega_0 - \mathrm{i}\frac{\Gamma}{2}\right)}. \tag{10.29}$$

Using the fact that

$$\int \mathrm{d}t_j \, \mathrm{e}^{\mathrm{i}(\omega_\ell - \omega_{\ell'})t_j} = 2\pi \, \delta(\omega_\ell - \omega_{\ell'}), \tag{10.30}$$

we obtain

$$\begin{aligned}\sum_j |1(t_j)\rangle\langle 1(t_j)| &= \rho_j \int \mathrm{d}\omega_\ell \frac{[\rho(\omega_\ell)]^2 |K_1|^2}{(\omega_\ell - \omega_0)^2 + \Gamma^2/4} \\ &= \rho_j [\rho(\omega_0)]^2 |K_1|^2 \frac{2\pi}{\Gamma}\end{aligned} \tag{10.31}$$

(as above, we take $\rho(\omega_\ell)$ constant over the bandwidth Γ around ω_0). Recalling (10.25), we finally have

$$\frac{1}{\rho_j \rho(\omega_0)} \sum_j |1(t_j)\rangle\langle 1(t_j)| = 1, \tag{10.32}$$

which can be used as a closure relation to expand single-photon states.

On the other hand, the $|1(t_j)\rangle$ only obey an approximate orthogonality relation:

$$\begin{aligned}\langle 1(t_j)|1(t_{j'})\rangle &= \sum_\ell \sum_{\ell'} \frac{|K_1|^2 \exp(\mathrm{i}\omega_\ell t_j)\exp(-\mathrm{i}\omega_{\ell'} t_{j'})}{\left(\omega_\ell - \omega_0 + \mathrm{i}\frac{\Gamma}{2}\right)\left(\omega_\ell - \omega_0 - \mathrm{i}\frac{\Gamma}{2}\right)}\langle 1_\ell|1_{\ell'}\rangle \\ &= \sum_\ell \frac{|K_1|^2 \exp[\mathrm{i}\omega_\ell(t_j - t_{j'})]}{(\omega_\ell - \omega_0)^2 + \Gamma^2/4} = |K_1|^2\rho(\omega_0) \\ &\quad \times \int \mathrm{d}\omega_\ell \frac{\mathrm{e}^{\mathrm{i}\omega_\ell(t_j - t_{j'})}}{(\omega_\ell - \omega_0)^2 + \Gamma^2/4} \\ &= \frac{2\pi}{\Gamma}|K_1|^2\rho(\omega_0)\mathrm{e}^{\mathrm{i}\omega_0(t_j - t_{j'})}\mathrm{e}^{-\frac{\Gamma}{2}|t_j - t_{j'}|}. \end{aligned} \tag{10.33}$$

Using (10.25) once more, we find

$$\langle 1(t_j)|1(t_{j'})\rangle = \mathrm{e}^{\mathrm{i}\omega_0(t_j - t_{j'})}\mathrm{e}^{-\frac{\Gamma}{2}|t_j - t_{j'}|}. \tag{10.34}$$

This relation, as well as the closure relation (10.32), show that the ensemble of states $|1(t_j)\rangle$ is an overcomplete basis [12]. This is used in Section 10.2.7.

Remark. To obtain a result that is meaningful for a real experiment, we need to take into account the transverse profile of the light beam. A simple model that captures all the necessary features makes use of "top hat" modes, transversely homogeneous over a surface S, and with an arbitrary length L (along $\mathbf{u}$) (see for instance [17, Section 5B.1.2]). We have then

$$\left[\mathcal{E}_\omega^{(1)}\right]^2 = \frac{\hbar\omega}{2\varepsilon_0 LS} \tag{10.35}$$

$$\rho(\omega) = \frac{L}{2\pi c}. \tag{10.36}$$

Substituting in (10.26), we obtain an expression independent of L

$$E_0 = \sqrt{\frac{\hbar\omega_0}{2\varepsilon_0 Sc\Gamma^{-1}}}. \tag{10.37}$$

Note that this is the amplitude for a single photon in a volume $Sc\Gamma^{-1}$.

If the detector covers the whole beam, we must integrate $w^{(1)}$ [Eq. (10.24)] over S to obtain the probability of detection per unit time at position $\mathbf{r} = 0$, and we get

$$\frac{\mathrm{d}\mathcal{P}^{(1)}}{\mathrm{d}t} = \eta\frac{\hbar\omega_0}{2\varepsilon_0 c\Gamma^{-1}}\mathrm{H}\left(t - t_j\right)\exp[-\Gamma(t - t_j)]. \tag{10.38}$$

A perfect photodetector should detect a single photon with a probability of 1, i.e.,

$$\int \mathrm{d}t \frac{\mathrm{d}\mathcal{P}^{(1)}}{\mathrm{d}t} = s\frac{\hbar\omega}{2\epsilon_0 c} = 1. \tag{10.39}$$

Hence, its sensitivity (in units of [electric field]$^{-2}$) per unit surface is

$$s_{\text{perfect}} = \frac{2\varepsilon_0 c}{\hbar\omega}. \tag{10.40}$$

10.2.4 Quasi-Classical Wavepacket

A fundamental reason for the success of the semi-classical model of matter-light interaction is the fact that most of the light sources available in everyday life, or even in laboratories, deliver light beams whose behavior can be fully described by the semi-classical model. In particular, the rates of single and joint photodetections can be expressed in terms of Eqs. (10.15) and (10.16). This can be understood, in the fully quantum optics formalism, by the fact that such light beams can be described by quantum states of radiation called *coherent states* or *quasi-classical states* [11,12]. A quasi-classical state $|\alpha_\ell\rangle$ of the mode ℓ is an eigenstate of the destruction operator $\hat{a}_\ell$

$$\hat{a}_\ell|\alpha_\ell\rangle = \alpha_\ell|\alpha_\ell\rangle, \tag{10.41}$$

with α_ℓ a complex number. A multimode quasi-classical state is

$$|\Psi_{\rm qc}\rangle = |\alpha_{\ell=1}\rangle \otimes |\alpha_{\ell=2}\rangle \otimes \cdots \otimes |\alpha_\ell\rangle \otimes \cdots \tag{10.42}$$

This state is an eigenstate of the positive-frequency electric-field operator (10.1):

$$\hat{\mathbf{E}}^{(+)}(\mathbf{r},t)|\Psi_{\rm qc}\rangle = \mathbf{E}^{(+)}_{\rm cl}(\mathbf{r},t)|\Psi_{\rm qc}\rangle \tag{10.43}$$

with the eigenvalue

$$\mathbf{E}^{(+)}_{\rm cl}(\mathbf{r},t) = \mathrm{i}\sum_\ell \mathcal{E}^{(1)}_\ell \alpha_\ell \overrightarrow{\varepsilon_\ell}\, \exp\{\mathrm{i}(\mathbf{k}_\ell \cdot \mathbf{r} - \omega_\ell t)\}. \tag{10.44}$$

It turns out that $\mathbf{E}^{(+)}_{\rm cl}(\mathbf{r},t)$ is the positive frequencies part of a classical field that we can associate with $|\Psi_{\rm qc}\rangle$. One can then check by simple inspection that the rates of simple or double photodetection (10.11) or (10.13) obtained for the state (10.42) are identical to the ones obtained using the semi-classical expressions (10.15) and (10.16) with the classical field (10.44).

Such quasi-classical states—or, more generally, a statistical ensemble of states of the form (10.42)—allow one to describe, in the quantum optics formalism, the light emitted by what we will thus call *classical sources*, for instance a thermal source, or a laser operated well above threshold (see Section 10.2.6). But they also allow us to build quasi-classical wavepackets that lead to the same probability of single detections as the one-photon wavepackets considered in Section 10.2.3. To show this, we take again the case of propagation along $\mathbf{u}$

$$\mathbf{k}_\ell = \mathbf{u}\frac{\omega_\ell}{c}, \tag{10.45}$$

with a single polarization

$$\overrightarrow{\varepsilon_\ell} = \overrightarrow{\varepsilon}. \tag{10.46}$$

We then assume the α_ℓ's have a distribution

$$\alpha_\ell = \frac{K_{\rm qc}}{\omega_\ell - \omega_0 + \mathrm{i}\Gamma/2}, \tag{10.47}$$

and we take $K_{\rm qc}$ to be real, for simplicity. We can then calculate explicitly the quasi-classical field (10.44). As in Section 10.2.3, we replace the sum by an integral, using the density of states $\rho(\omega)$. Integration in the complex plane yields

$$\mathbf{E}_{\rm cl}^{(+)}(\mathbf{r},t) = \overrightarrow{\varepsilon}\, E_0 \mathrm{H}\left(t - \frac{\mathbf{r}\cdot\mathbf{u}}{c}\right) \exp\left\{-\frac{\Gamma}{2}\left(t - \frac{\mathbf{r}\cdot\mathbf{u}}{c}\right)\right\} \exp\left\{-\mathrm{i}\omega_0\left(t - \frac{\mathbf{r}\cdot\mathbf{u}}{c}\right)\right\} \tag{10.48}$$

with

$$E_0 = -\mathrm{i}\, 2\pi\rho(\omega_0)\mathcal{E}_{\omega_0}^{(1)} K_{\rm qc}. \tag{10.49}$$

Since $\mathbf{E}_{\rm cl}^{(+)}$ is the eigenvalue of $\hat{\mathbf{E}}^{(+)}$ associated with the radiation state (10.42), the rate of single photodetections (10.11) can be written as

$$w^{(1)}(\mathbf{r},t) = \eta|\mathbf{E}_{\rm c}(\mathbf{r},t)|^2 = \eta|E_0|^2 \mathrm{H}\left(t - \frac{\mathbf{r}\cdot\mathbf{u}}{c}\right) \exp\left\{-\Gamma\left(t - \frac{\mathbf{r}\cdot\mathbf{u}}{c}\right)\right\}. \tag{10.50}$$

Like (10.24) (with t replaced by $t - \mathbf{r}\cdot\mathbf{u}/c$), Eq. (10.50) suggests the propagation of a wavepacket damped with a time constant Γ^{-1}. However, the quasi-classical wavepacket introduced here differs in many aspects from the one-photon wavepacket of Section 10.2.3. The most striking difference can be seen in Section 10.2.5. Here, we note that the quasi-classical state $|\Psi_{\rm qc}\rangle$ is not an eigenstate of the number of photons operator $\hat{N}$. More precisely, it can be shown that if we were to measure the photon number in such a state, we would find a Poisson distribution. One can readily calculate the average of that distribution, i.e., the average photon number

$$\langle N\rangle_{\rm qc} = \langle\Psi_{\rm qc}|\hat{N}|\Psi_{\rm qc}\rangle = \sum_{\ell} |\alpha_\ell|^2, \tag{10.51}$$

and its standard deviation

$$\langle\Delta N\rangle_{\rm qc} = \left[\langle\hat{N}^2\rangle - (\langle\hat{N}\rangle)^2\right]^{1/2} = \left[\langle N\rangle_{\rm qc}\right]^{1/2}. \tag{10.52}$$

Using a method similar to the one yielding Eq. (10.25), we can express (10.51) as

$$\langle N\rangle_{\rm qc} = \int \mathrm{d}\omega\, \rho(\omega) \frac{|K_{\rm qc}|^2}{(\omega-\omega_0)^2 + \Gamma^2/4} = \frac{2\pi}{\Gamma}\rho(\omega_0)|K_{\rm qc}|^2. \tag{10.53}$$

It is important to realize that the constant $K_{\rm qc}$ (or equivalently, the average photon number) can be chosen arbitrarily (contrary to constant K_1 in the case of a one-photon wavepacket). A quasi-classical wavepacket thus can be built with any average photon number. In particular, $K_{\rm qc}$ can be chosen small enough to get an average photon number smaller than one. Such a state is the quantum description of a quasi-classical pulse that has been strongly attenuated by a neutral density filter.

Remark. Using the results above, we find that the amplitude E_0 of Eq. (10.49) assumes a form similar to (10.26), with the right-hand side multiplied by $[\langle N\rangle_{\rm qc}]^{1/2}$

$$E_0 = -\mathrm{i}[\langle N\rangle_{\rm qc}]^{1/2}\mathcal{E}^{(1)}_{\omega_0}[2\pi\ \rho(\omega_0)\Gamma]^{1/2}\mathrm{e}^{-\mathrm{i}\omega_0 t_0}. \tag{10.54}$$

Taking the same set of top-hat modes as in the remark of Section 10.2.3, we find a rate of photodetection

$$w^{(1)}(\mathbf{r},t) = s\frac{\hbar\omega}{2\varepsilon_0 c}\frac{\Gamma}{S}\langle N\rangle_{\rm qc}\mathrm{H}\left(t-\frac{\mathbf{r}\cdot\mathbf{u}}{c}\right)\exp\left\{-\Gamma\left(t-\frac{\mathbf{r}\cdot\mathbf{u}}{c}\right)\right\}. \tag{10.55}$$

An integration over the whole section S of the beam, and over time, yields the average number of photoelectrons

$$\iint \mathrm{d}^2S\int \mathrm{d}t\ w^{(1)}(\mathbf{r},t) = s\frac{\hbar\omega}{2\varepsilon_0 c}\langle N\rangle_{\rm qc}. \tag{10.56}$$

For a perfect detector, of sensitivity given by (10.40), the average number of counts is equal to the average number of photon $\langle N\rangle_{\rm qc}$, as expected.

10.2.5 The Possibility of an Experimental Distinction

We now compare the predictions of quantum optics for a one-photon wavepacket and for a quasi-classical wavepacket. Equations (10.24) and (10.50) show that if we measure the instants of photodetection for wavepackets whose time of emission is known, and build the histogram of the delays between the emission and the photodetection, the results for single-photon wavepackets and quasi-classical wavepackets are similar. Measurements of $w^{(1)}(\mathbf{r},t)$ therefore do not allow us to distinguish between a one-photon wavepacket and a quasi-classical wavepacket. Actually, it is well known that when a distinction between classical light and quantum light is possible, it cannot be observed on single detection signals, but rather on double detection signals [34]. We thus calculate the probability of double detections for both cases.

In the case of a quasi-classical wavepacket of the form (10.42), we again use the fact that it is an eigenstate of $\hat{\mathbf{E}}^{(+)}(\mathbf{r},t)$ and obtain from (10.13)

$$w^{(2)}(\mathbf{r},t;\mathbf{r}',t') = \eta^2|\mathbf{E}_{\rm cl}(\mathbf{r},t)|^2|\mathbf{E}_{\rm c}(\mathbf{r}',t')|^2. \tag{10.57}$$

The probability of a double detection is the product of the probabilities of the single detections. The detection events are uncorrelated. This is the same result as would be obtained in the semi-classical model of matter-light interaction, for a wavepacket with Fourier components distributed as the α_ℓ's.

Let us now consider the case of a single-photon wavepacket of the form (10.17). We have now

$$\hat{\mathbf{E}}^{(+)}(\mathbf{r},t)|1\rangle = \left[\sum_\ell \overrightarrow{\varepsilon_\ell}\mathcal{E}^{(1)}_\ell c_\ell \exp\left\{\mathrm{i}\omega_\ell\left(\frac{\mathbf{r}\cdot\mathbf{u}}{c}-t\right)\right\}\right]|0\rangle \tag{10.58}$$

and therefore

$$\hat{\mathbf{E}}^{(+)}(\mathbf{r}',t')\hat{\mathbf{E}}^{(+)}(\mathbf{r},t)|1\rangle = 0 \tag{10.59}$$

since $\hat{a}_\ell|0\rangle = 0$. We conclude that

$$w^{(2)}(\mathbf{r},t;\mathbf{r}',t') = 0. \tag{10.60}$$

The probability of a double detection is thus strictly null in the case of a single-photon wavepacket. This property ("*anticorrelation*") is not surprising if one remembers that the number of photons is a good quantum number, and its value is 1. Since a photodetection amounts to destroying a photon, there is no photon left to allow for a second detection.

In contrast, in a semi-classical wavepacket the number of photons is not a good quantum number, since $|\Psi_{\text{qc}}\rangle$ is not an eigenstate of $\hat{N}$, and the probability to have two photons is not null. It is therefore not surprising that one can have two photodetections.

This difference allows one to make an experimental distinction between a true single-photon wavepacket, and a quasi-classical wavepacket, even when attenuated enough that the average number of photons is much less than 1. One can then ask: can such a difference be observed, when one takes into account experimental inefficiencies and noise? We will see in Section 10.3 that it is indeed possible to establish a quantitative criterion that renders the distinction presented above fully operational, leading to practical tests in realistic experiments. But before addressing that question, we will ask, still from a theoretical point of view, whether various kinds of strongly attenuated light beams may exhibit an anomalously small rate of double photodetection, by comparison to what is expected for a classical wave.

10.2.6 Attenuated Continuous Light Beams

In this subsection, we consider the case of a continuous beam emitted by a CW laser, or even a thermal source, attenuated to the point where the average power is so weak that if we insist to describe the beam as made of photons, the average distance between these photons would be large compared to a standard interferometric system (say several meters).

Let us start with the simplest case, the beam emitted by a perfectly stable single-mode laser, of average power P_{Laser}. It is well known [34] that such a beam is well described by a quasi-classical state $|\alpha_{\text{Laser}}\rangle$ of the mode associated with the laser beam. Even in an ideal laser, the complex number α_{Laser} has some fluctuations due to spontaneous emission [38], but the fluctuations of the modulus $|\alpha_{\text{Laser}}|$ can be considered negligible, provided the laser operates well above threshold.

A laser beam has a non-uniform transverse profile (for instance, a Gaussian profile for the fundamental transverse mode), and one should use the corresponding non-uniform modes of the electromagnetic field to correctly

describe the quantized field associated with the laser beam. To simplify, we use again the top-hat modes introduced in the remark of Section 10.2.3, with a transverse profile uniform over an area S_{Laser}. The volume of quantization is then $S_{\text{Laser}} \times L$, where L is an arbitrary length along the beam axis, which can be taken as large as necessary. The single-photon amplitude $\mathcal{E}^{(1)}_{\text{Laser}}$ then assumes the value (10.35) with S replaced by S_{Laser}, and the density of modes has the value (10.36). The modulus of α_{Laser} is related to the average number of photons in the quantization volume by

$$\langle N \rangle_{\text{qc}} = |\alpha_{\text{Laser}}|^2 = \frac{P_{\text{Laser}}}{\hbar\omega_{\text{Laser}}} \frac{L}{c}. \tag{10.61}$$

Since $|\alpha_{\text{Laser}}\rangle$ is an eigenstate of the positive-frequency electric-field operator (10.1), the calculation of the single and joint photodetections is trivial (cf. Section 10.2.4). The rate of single photodetections is uniform in the profile, and is equal to

$$w^{(1)}(\mathbf{r},t) = \eta \left[\mathcal{E}^{(1)}_{\ell}\right]^2 |\alpha_{\text{Laser}}|^2. \tag{10.62}$$

Replacing $\mathcal{E}^{(1)}_{\ell}$ by its value, and assuming a perfect detector, we obtain

$$w^{(1)}(\mathbf{r},t) = \eta_{\text{perfect}} \frac{\hbar\omega}{2\varepsilon_0 L S} |\alpha_{\text{Laser}}|^2 = |\alpha_{\text{Laser}}|^2 \frac{c}{L}, \tag{10.63}$$

i.e., according to (10.61), the average number of photons per unit time, as it should be.

The density of double detections is also uniform

$$w^{(2)}(\mathbf{r},t;\mathbf{r}',t') = \eta^2 \left[\mathcal{E}^{(1)}_{\ell}\right]^4 |\alpha_{\text{Laser}}|^4. \tag{10.64}$$

Moreover, we see that

$$w^{(2)}(\mathbf{r},t;\mathbf{r}',t') = w^{(1)}(\mathbf{r},t) \cdot w^{(1)}(\mathbf{r}',t'). \tag{10.65}$$

This means that the detection events are independent from each other. If we take a perfect photodetector that detects every photon, we thus conclude that the photons are randomly distributed in time with a uniform probability density. This property remains true even for an attenuated beam, whatever the level of attenuation, since this only amounts to reducing the magnitude $|\alpha_{\text{Laser}}|$. This property is equivalent to the fact that if one looks for the statistics of photodetections in a given time interval, we expect to find a Poisson distribution.

If now we consider thermal light, it can be considered constituted by a statistical ensemble of quasi-classical states associated with a continuum of modes of the electromagnetic field. Reasoning as in Section 10.2.5, the calculation can be done using the semi-classical model of matter-light interaction, for a classical stochastic field [39]. One can then show, using

a standard Cauchy-Schwartz inequality, that the rates of single and double photodetections, calculated according to formulae (10.15) and (10.16), obey the relation

$$w^{(2)}(\mathbf{r},t;\mathbf{r},t) \geq (w^{(1)}(\mathbf{r},t))^2. \tag{10.66}$$

We can thus conclude that such light beams, even strongly attenuated, never lead to a null rate of double detection. The situation is thus explicitly different from what happens with genuine single-photon wavepackets (Section 10.2.5). This conclusion remains valid when we use the criterion that is derived in Section 10.3.3, which applies to real experiments.

10.2.7 Light From a Discharge Lamp

We consider now light emitted by a source constituted of many independent emitters, each emitting one-photon wavepacket, at random times. The light is collimated, and we can thus describe the radiation state as constituted of many independent one-photon wavepackets introduced in Section 10.2.3. We call μ the average number of single photons per unit time, and we consider a time interval T in which we have $N = \mu T$ wavepackets. We will then write the radiation state as

$$|\Psi_N\rangle = |1(t_1)\rangle \otimes |1(t_2)\rangle \cdots \otimes |1(t_N)\rangle. \tag{10.67}$$

In writing this expression, which reflects the fact that the one-photon wavepackets are independent, we assume that the $|1(t_j)\rangle$ states are orthogonal, i.e., the second member of Eq. (10.34) is replaced by $\delta_{jj'}$. This is reasonable if the wavepackets are produced by the same emitter (since then there is a delay between them), or if they are emitted by different emitters with frequencies ω_0 that are not exactly the same because of Doppler effect or inhomogeneous broadening.

The ensemble of the one-photon states $\{|1(t_1)\rangle, \ldots, |1(t_N)\rangle\}$ can then be considered a basis for the Fock space of any combination of such one-photon states. It is then convenient to define creation and destruction operators $\hat{a}^\dagger(t_\ell)$ and $\hat{a}(t_\ell)$ $(\ell = 1, \ldots, N)$ such that

$$\hat{a}^\dagger(t_\ell)|0\rangle = |1(t_\ell)\rangle \tag{10.68}$$

and

$$\left[\hat{a}(t_\ell), \hat{a}^\dagger(t_{\ell'})\right] = \delta_{\ell\ell'}. \tag{10.69}$$

The state (10.67) can then be written as

$$|\Psi_N\rangle = \hat{a}^\dagger(t_1)\hat{a}^\dagger(t_2)\ldots\hat{a}^\dagger(t_n)|0\rangle. \tag{10.70}$$

The restriction of the electric-field operator $\hat{\mathbf{E}}^{(+)}(\mathbf{r},t)$ to that space can be written as

$$\hat{\mathbf{E}}_N^{(+)}(\mathbf{r},t) = \overrightarrow{\varepsilon} \sum_{\ell=1}^{N} E_{t_\ell}^{(1)}(t)\hat{a}(t_\ell). \tag{10.71}$$

To determine the probability of a single detection per unit time, we need to calculate

$$\begin{aligned}\hat{\mathbf{E}}_N^{(+)}(0,t)|\Psi_N\rangle &= \overrightarrow{\varepsilon}\, E_{t_1}^{(1)}(t)|1(t_2)\rangle \otimes |1(t_3)\rangle \otimes \cdots \otimes |1(t_N)\rangle \\ &\quad + \overrightarrow{\varepsilon}\, E_{t_2}^{(1)}(t)|1(t_1)\rangle \otimes |1(t_3)\rangle \otimes \cdots \\ &\quad + \cdots \\ &= \overrightarrow{\varepsilon} \sum_{\ell=1}^{N} E_{t_\ell}^{(1)} \underbrace{\bigotimes_{j\neq\ell} |1(t_j)\rangle}_{N-1 \text{ terms}}. \end{aligned} \tag{10.72}$$

The state above is a state with $N-1$ photons. Taking its modulus and using (10.24), we obtain

$$\begin{aligned} w^{(1)}(0,t) &= \eta \sum_{\ell=1}^{N} |E_{t_\ell}^{(1)}(t)|^2 \\ &= \eta |E_0|^2 \sum_{\ell=1}^{N} \mathrm{H}(t-t_\ell)\exp[-\Gamma(t-t_\ell)]. \end{aligned} \tag{10.73}$$

Actually, with such a source we cannot measure the quantity above, since even for an ideal detector we have at most one detection per wavepacket. If we repeat the experiment, and select another interval with N one-photon wavepackets, the distribution of the times $\{t_1,\ldots,t_\ell,t_N\}$ will be different, so that the result after a large number of such experiments is obtained by averaging over each t_ℓ distributed uniformly in the interval $T = N\mu^{-1}$. The result of that averaging is constant in time

$$\overline{w^{(1)}} = \eta |E_0|^2 \mu \Gamma^{-1}. \tag{10.74}$$

Integrating over the whole area of an ideal detector, and reasoning as in Eqs. 10.35–10.40, we obtain an average probability of detection per unit time

$$\frac{\overline{\mathrm{d}\mathcal{P}^{(1)}}}{\mathrm{d}t} = \mu. \tag{10.75}$$

To evaluate the probability of double detection, we apply the operator $\hat{\mathbf{E}}_N^{(+)}$ to (10.72):

$$\sum_{\ell=1}^{N} E_{t_\ell}^{(1)}(t) \sum_{p\neq\ell} E_{t_p}^{(1)}(t) \underbrace{\bigotimes_{j\neq p,\ell} |1(t_j)\rangle}_{N-2 \text{ terms}}. \tag{10.76}$$

In the sum above, the two terms obtained by exchanging ℓ and p are identical, and we can thus write

$$\hat{\mathbf{E}}_N^{(+)}(0,t)\hat{\mathbf{E}}_N^{(+)}(0,t)|\Psi_N\rangle = 2\sum_{\ell=1}^{N} E_{t_\ell}^{(1)}(t) \sum_{p>\ell} E_{t_p}^{(1)}(t) \bigotimes_{j\neq p,\ell} |1,t_j\rangle. \tag{10.77}$$

Taking its square modulus, we obtain

$$w^{(2)}(t,t) = 4\eta^2 \sum_{\ell=1}^{N} \sum_{p>\ell} |E^{(1)}(t_\ell)|^2 |E^{(1)}(t_p)|^2. \tag{10.78}$$

We again average over all t_ℓ and t_p in the interval T, and we obtain

$$\overline{w^{(2)}(t,t)} = 2\frac{N(N-1)}{N^2}\left[\overline{w^{(1)}}\right]^2, \tag{10.79}$$

where $\overline{w^{(1)}}$ is given in (10.74). If the number of photons is large enough, we have $\overline{w^{(2)}} = 2\left[\overline{w^{(1)}}\right]^2$. The factor 2 is the celebrated Hanbury Brown and Twiss factor.

We thus find that there is no possibility to observe an anticorrelation effect with light emitted from a discharge lamp, even if the one-photon wavepackets are well separated from each other. The reason is that the various wavepackets are emitted at random times independent from each other, and there is a significant probability to have two wavepackets arriving at the same time.

Remark. If we make $N = 1$ in Eq. (10.79), we find $\overline{w^{(2)}} = 0$. It does not mean that if we take a small enough time interval we can expect to observe $\overline{w^{(2)}} = 0$. Indeed, for a source emitting one-photon wavepackets at random times the number N is not strictly fixed, it is in fact distributed according to a Poisson law. A calculation averaging over that distribution would give $\overline{w^{(2)}}(t,t) = 2\left[\overline{w^{(1)}}\right]^2$, whatever the interval.

10.2.8 Conclusion: What is Single-Photon Light?

In this section, we have shown that a genuine single-photon wavepacket, i.e., a one-photon state emitted at a well-known time, exhibits a characteristic behavior, the fact that it cannot be detected jointly by two photodetectors (anticorrelation). Such a behavior is not expected in the case of an attenuated beam from a classical lamp, including the case of a discharge lamp where one has single-photon wavepackets shorter than the average time between the wavepackets. The paradoxical behavior in the latter case is resolved when we realize that the problem is the fact that one has no information about the time when any single-photon wavepacket is emitted. We can thus conclude that it is not enough to have single-photon wavepackets to have single-photon light. We need in addition to know *at which time each single-photon wavepacket is emitted* [40]. This is the case for the two types of sources described below: *heralded single-photon sources* on the one hand, and *on-demand single-photon sources* on the other hand.

10.3 PHOTON PAIRS AS A RESOURCE FOR SINGLE PHOTONS

10.3.1 Introduction

When an atom emits from an excited level, the fluorescent light emitted is a one-photon wavepacket, as can be guessed merely from energy conservation. However, in usual sources, such as discharge lamps, many excited atoms are seen simultaneously by a detector, and their time of excitation is random (Section 10.2.7). The theoretical description of the light then is a mixture of one-photon wavepackets of the form presented in Section 10.2, with random leading-edge times. If one also takes into account the fluctuations of the number of excited atoms, the emitted light can be considered a statistical ensemble of quasi-classical states, and in this situation there is no hope to observe any non-classical effects. To observe non-classical properties in fluorescent light, it is necessary to isolate single-atom emissions, either in space, or in time. This can be done in sources of "heralded" single photons, based on the emission of separated pairs of photons: the first photon then "heralds" the emission of the second one, allowing one to isolate single-atom emission in time.

The production of pairs of photons occurs in many different contexts in physics, including particle physics (e.g., the electron-positron annihilation, producing two γ photons), nuclear physics and atomic physics (through cascade de-excitation between several levels), and non-linear optics (pair production in spontaneous parametric fluorescence). In the latter case, the temporal correlation between the two photons of one pair, a fully quantum property, was observed first in 1970 by Burnham and Weinberg [6] and studied more accurately by Hong *et al.* [41], while the specifically quantum properties of the photon pairs emitted by an atomic cascade were demonstrated in 1974 by Clauser (see Section 10.3.2).

However, it took some time to realize that a very simple way to understand these specifically quantum properties is to consider the quantum state of the light for the second photon only, once the first one has been detected: according to the "projection postulate" of quantum mechanics this second photon is in a state very close to a one-photon state, or more precisely, a one-photon wavepacket with a well-defined leading-edge time (or peak time). One can say that the second photon is "heralded" by the detection of the first [9]. This expression has become popular and is now used as a generic name for such sources.

In this section, we first present and discuss inequalities that apply to "classical" light, i.e., light described by the standard wave model of classical optics, or equivalently light described by the quantum theory as a statistical mixture of quasi-classical states. Such inequalities are derived for the case of an atomic cascade (Section 10.3.2), and for a single photon on a beamsplitter (Section 10.3.3). These inequalities are fully general in the classical context, and since quantum light can contradict them, they delineate a limit beyond which "specifically quantum effects" can be observed. In Section 10.3.4, we

present the anticorrelation experiment that allowed us to conclude that our 1986 source was a true single-photon source, and we contrast this result with the one obtained with strongly attenuated classical light pulses.

10.3.2 Non-Classical Properties in an Atomic Cascade

In 1974, John Clauser proposed a scheme to obtain a "model-independent" inequality applying to any classical description of pairs of photons emitted by an atomic radiative cascade [3]. His idea was to "split" simultaneously both the first and second photons of the cascade, by collecting the light emitted on opposite sides of an assembly of excited atoms, and focusing it separately into two beams. The wavelength λ_1 on one side was selected to correspond to that of the first transition of the cascade, and that on the other, λ_2, to the second. The two light beams impinged on beamsplitters, thus creating a total of four beams, between which coincidence rates of photodetections are measured. The semi-classical expression of a coincidence rate between detectors i and j is (see Eq. (10.16))

$$C_{ij} = \eta_i \eta_j T^{-1} \int_{-T/2}^{T/2} \int_{-T/2}^{T/2} \langle I_i(t+t') I_j(t+t'') \rangle dt' \, dt'', \tag{10.80}$$

where η_i, η_j are the detection efficiencies of the photodetectors, and I_i (respectively I_j) the classical light intensity $I_i = |\mathbf{E}_i^{(+)}(\mathbf{t})|^2$ at photodetector i (respectively j). The time integral bears over the duration T of the run, while the brackets denote a statistical average over many runs.

By using four photomultipliers labeled $\gamma_{1A}, \gamma_{1B}, \gamma_{2A}$, and γ_{2B}, the coincidence rates were monitored between the four combinations: $\gamma_{1A} - \gamma_{1B}, \gamma_{2A} - \gamma_{2B}, \gamma_{1A} - \gamma_{2B}$, and $\gamma_{2A} - \gamma_{1B}$. A diagram of the arrangement is shown in Fig. 10.2. Defining $I_1(t)$ and $I_2(t)$ as the instantaneous light intensities at the $\gamma_{1A} - \gamma_{1B}$ beam splitter with wavelength λ_1, and at the $\gamma_{2A} - \gamma_{2B}$ beam splitter with wavelength λ_2, respectively, it follows directly from the Cauchy-Schwarz inequality that the following inequality holds:

$$\begin{aligned} &\left[\int_{-T/2}^{T/2} \int_{-T/2}^{T/2} \langle I_1(t+t'+\tau_1) I_1(t+t''+\tau_1) \rangle dt' \, dt'' \right] \\ &\left[\int_{-T/2}^{T/2} \int_{-T/2}^{T/2} \langle I_2(t+t'+\tau_2) I_2(t+t''+\tau_2) \rangle dt' \, dt'' \right] \\ \geqslant &\left[\int_{-T/2}^{T/2} \int_{-T/2}^{T/2} \langle I_1(t+t'+\tau_1) I_2(t+t''+\tau_2) \rangle dt' \, dt'' \right]^2 . \end{aligned}$$

Using the definition (10.80) of C_{ij}, this can be written as

$$C_{1A-1B}(0) C_{2A-2B}(0) \geqslant C_{1A-2B}(\tau) C_{1B-2A}(\tau). \tag{10.81}$$

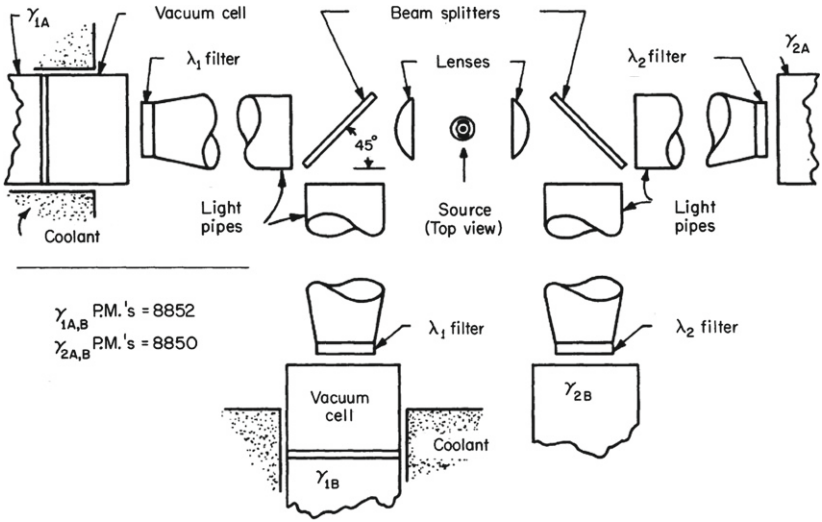

FIGURE 10.2 Schematic diagram of the apparatus used in John Clauser's 1974 experiment.

This simple calculation ignores a possible polarization dependence of the detectors, and the finite photocathode areas, as well as the nonvanishing phototube dark rates (c.f. Chapter 3). However, it can be shown that the above inequality is fully general and holds for these cases as well.

From a quantum point of view, the coincidence rates C_{1A-2B} and C_{2A-1B} are due to the strong temporal correlation between the two photons in each pair emitted by the cascade, and these coincidence rates can reach quite high values. On the other hand, the rates C_{1A-1B} and C_{2A-2B} require random coincidences between photons emitted by different atoms, and for a low-density source, such coincidence rates are much smaller than C_{1A-2B} and C_{2A-1B}. Therefore the above equality can be violated by a large amount, as has been confirmed by the experiment [3].

10.3.3 Anticorrelation for a Single Photon on a Beamsplitter

The main idea of the previous experiment is thus to compare "intra-beam" correlations (auto-correlations), and "inter-beam" correlations (cross-correlations), the first ones being always larger for classical beams, whereas the opposite situation happens for the quantum light emitted by an atomic cascade. This approach, however, does not directly exhibit the anticorrelation behavior that is only associated with a single photon. This is why we introduced the scheme of Fig. 10.3. In that scheme [42], the detection of the first photon of a radiative cascade fires a trigger that generates an electronic gate of duration τ_{gate}, synchronized with, and somewhat longer than, the decay constant Γ^{-1} of the one-photon wavepacket associated with the second photon of the cascade.

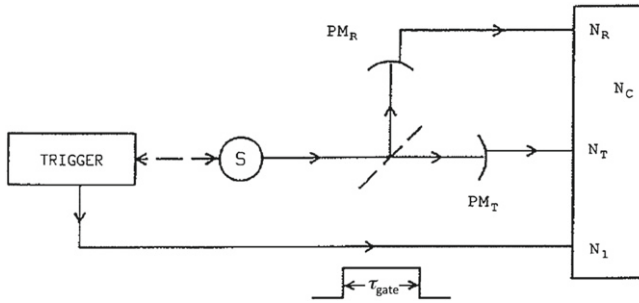

FIGURE 10.3 Experiment to look for an anticorrelation on a beam splitter. The source S emits light pulses that fall on a beam splitter and can be detected in both channels (reflected and transmitted) behind the beam splitter. The detectors are enabled during a gate τ_{gate} synchronized with the light pulses. The rates of single detection (N_R and N_T) and coincidence (N_C) are monitored. If the light pulse contains only one photon, one detection is expected at most, and no coincidence is expected: this is the anticorrelation effect. In sources of heralded single photons based on photon pairs, such as the ones emitted by the radiative cascade of Fig. 10.4, the trigger is activated by the detection of the other photon of the pair.

That single-photon wavepacket is launched toward a beamsplitter with two detectors in the transmitted and reflected legs, and these detectors are enabled only during the gates associated with the trigger, i.e., during the time interval corresponding to the single-photon wavepacket. If both detectors fire during the same gate, a coincidence is recorded. A counting system monitors the triggering events, the detection events, and the coincidences.

Consider an experiment that consists of running the source for a given duration and counting the total number of counts in the transmitted (N_T) or reflected (N_R) channels, the total number of coincidences (N_c), and the total number of gates N_1. We can then estimate the probabilities of single detections per gate,

$$P_R = \frac{N_R}{N_1} \quad \text{and} \quad P_T = \frac{N_T}{N_1}, \tag{10.82}$$

and the probability of a coincidence per gate,

$$P_c = \frac{N_c}{N_1}. \tag{10.83}$$

According to our intuition, we expect P_c to be zero in the ideal case of a one-photon wavepacket, and to be non-zero for a classical light pulse. As in the previous section, this discussion can be rephrased in the context of a comparison between the quantum theory of light and the semi-classical theories of light.

To establish classical inequalities, two equivalent approaches are possible: one is to consider the quantum state "heralded" by the first detection, and to look to the single and coincidence detections on both sides of the beamsplitter; the other one is to look "globally" at the cascade, so that a detection on one

side of the beamsplitter is already a coincidence (between the "heralding" and "heralded" photons), whereas clicks on both sides of the beamsplitter will be a "triple" coincidence.

In the first approach, we define

$$\Omega = \tau_{\text{gate}}^{-1} \int_0^{\tau_{\text{gate}}} I_B(t+t')dt'$$

as the time-averaged (classical) intensity impinging on the beamsplitter during the counting window τ_{gate}. For many pulses, one finds

$$P_R = s_R\overline{\Omega}, \quad P_T = s_T\overline{\Omega}, \quad P_c = s_R s_T\overline{\Omega^2},$$

where s_T and s_R are the global detection efficiencies (including the transmission and reflection coefficients of the beamsplitter) of each detector, and the overbar indicates a statistical average over many pulses. From the Cauchy-Schwarz inequality $\overline{\Omega^2} \geq (\overline{\Omega})^2$ one gets $P_c \geq P_R P_T$ or equivalently

$$N_c \geq \frac{N_R N_T}{N_1}.$$

In the second approach we consider the quantity, where ξ is a real variable:

$$\begin{aligned} F(\xi) &= \overline{I_A(t)\int_0^w \int_0^w (\xi + I_B(t+t'))(\xi + I_B(t+t''))dt'\,dt''} \\ &= \overline{I_A(t)\left(\int_0^w (\xi + I_B(t+t'))dt'\right)^2} \\ &= \xi^2 w^2 \overline{I_A(t)} + 2\xi w \overline{\int_0^w I_A(t)I_B(t+t')dt'} + \overline{I_A(t)\left(\int_0^w I_B(t+t')dt'\right)^2}. \end{aligned}$$

Since $F(\xi) \geq 0$, one obtains the usual Cauchy-Schwarz inequality:

$$\overline{I_A(t)} \times \overline{I_A(t)\left(\int_0^w I_B(t+t')dt'\right)^2} \geq \left(\overline{\int_0^w I_A(t)I_B(t+t')dt'}\right)^2$$

Reintroducing the appropriate detection-sensitivity factors $s_R s_T$ on both sides, one obtains:

$$N_1 N_c \geq N_R N_T,$$

which is the same as the inequality derived in the first approach. It is usually written

$$\alpha = \frac{P_c}{P_R P_T} = \frac{N_c N_1}{N_R N_T} \geq 1\,. \tag{10.84}$$

This inequality can be seen either as a property of the "heralded" wavepacket, or as a property of the correlation functions taking into account the "heralding"

event, corresponding to $I_A(t)$. Its physical content is very close to the inequality (10.66), and its violation (i.e., $\alpha < 1$), also called "anticorrelation" [5]. As for the antibunching effect [13], the observation of such an anticorrelation is an evidence against the semi-classical theories of light.

Remark. In the limit where τ_{gate} is very small, the inequality (10.84) is strictly equivalent to (10.66), or to $g^{(2)}(0) \geq 1$, where $g^{(2)}(\tau)$ is the usual normalized second-order correlation function [35]. So the condition $\alpha \geq 1$ can be seen as an "integrated" version of $g^{(2)}(0) \geq 1$, over a time window suited to the duration of the single-photon wavepacket. As for the semi-classical inequality $g^{(2)}(0) \geq 1$, or the semi-classical inequality $g^{(2)}(0) \geq g^{(2)}(\tau)$ used in [13], its violation has some relation with sub-Poissonian photon statistics, but no statistics are measured here, only intensity correlation functions. This is why we consider the wording "anticorrelation" well suited to characterize this violation.

10.3.4 The 1986 Anticorrelation Experiment

We have built an experiment corresponding to the scheme of Fig. 10.3, i.e., a setup allowing us to measure the single and coincidence rates on the two sides of a beamsplitter during the opening of gates triggered by events synchronous with the light pulses. This system has been used to study light pulses from a source designed to emit heralded one-photon wavepackets, i.e., based on pairs of photons emitted in a radiative cascade (see Section 10.3.4.1). But we have also used that setup to study strongly attenuated pulses from a classical source. (Section 10.3.4.2.)

10.3.4.1 Heralded One-Photon Pulses From an Atomic Cascade

Our source is composed of atoms excited to the upper level of a two-photon radiative cascade (Fig. 10.4) [4,5]. Each excited atom decays by emission of two photons at different frequencies ν_1 and ν_2. The time intervals between the detections of ν_1 and ν_2 are distributed according to an exponential law, corresponding to the decay time of the intermediate state (lifetime $\tau_s = 4.7$ ns, which is also the time constant Γ^{-1} of the wavepacket describing the heralded single photon ν_2). By choosing the rate of excitation much smaller than $(\tau_s)^{-1}$, we have cascades well separated in time. We use the detection of ν_1 as a trigger for a gate of duration $\tau_{\text{gate}} = 2\tau_s$, corresponding to the scheme of Fig. 10.3. During a gate, the probability of detecting a photon ν_2 coming from the atom that emitted ν_1 is much larger than the probability of detecting a photon ν_2 coming from any other atom in the source. We are then in a situation close to an ideal single-photon pulse, as defined in Section 10.2, and we expect the corresponding anticorrelation behavior on the beamsplitter.

The expected values of the counting rates can be obtained from a straightforward quantum mechanical calculation. Denoting N as the rate of excitation of the cascades, and η_1, η_T, and η_R as the detection efficiencies of

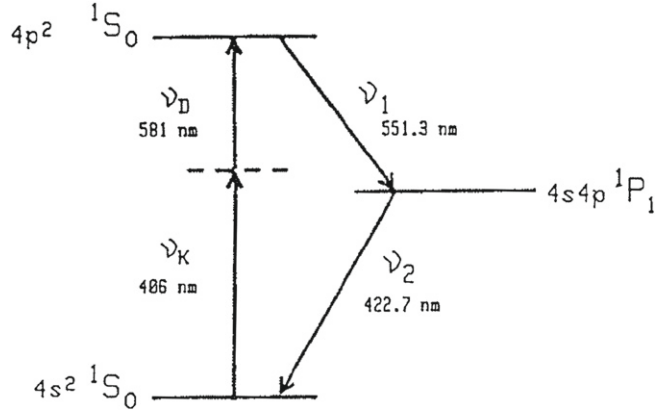

FIGURE 10.4 Radiative cascade in Calcium, used to produce heralded single-photon pulses. The atom is excited to the upper level of the cascade by a resonant two-photon excitation with a Krypton-ion laser and a tunable dye laser. It then re-emits photons ν_1 and ν_2. Detection of photon ν_1 activates the trigger of Fig. 10.3.

photons ν_1 and ν_2 (including the collection solid angles, optics transmissions, and detector efficiencies) we obtain:

$$N_1 = \eta_1 N, \tag{10.85}$$

$$N_T = N_1 \eta_T [f(\tau_{\text{gate}}) + N\tau_{\text{gate}}], \tag{10.86}$$

$$N_R = N_1 \eta_R [f(\tau_{\text{gate}}) + N\tau_{\text{gate}}], \tag{10.87}$$

$$N_c = N_1 \eta_T \eta_R [2f(\tau_{\text{gate}}) N\tau_{\text{gate}} + (N\tau_{\text{gate}})^2], \tag{10.88}$$

where $N\tau_{\text{gate}}$ is the probability to have a photon from another atom than the heralding atom, during the gate. The quantity $f(\tau_{\text{gate}})$, very close to 1 in this experiment, is the product of the factor $[1 - \exp(-\tau_{\text{gate}}/\tau_s)]$ (overlap between the gate and the exponential decay) and a factor somewhat greater than 1 that is related to the angular correlation between ν_1 and ν_2 [4,5].

The quantum mechanical prediction for α is

$$\alpha_{QM} = \frac{2f(\tau_{\text{gate}}) N\tau_{\text{gate}} + (N\tau_{\text{gate}})^2}{[f(\tau_{\text{gate}}) + N\tau_{\text{gate}}]^2}, \tag{10.89}$$

which is smaller than 1, as expected. The anticorrelation effect is strong (α small compared to 1) if $N\tau_{\text{gate}}$ is much smaller than 1. This condition is easily fulfilled if the cascades are well separated in time, in the average.

Counting electronics, including the gating system, was a critical part of this experiment. The gate τ_{gate} was realized by logical decisions based on the measurement of the time intervals between counts at the various detectors. This

TABLE 10.1 Feeble-Light Interference Experiments. All these Experiments have been Realized with Attenuated Light from a Usual Source

Author	Date	Interferometer	Detector	Photon Flux (s^{-1})	Interferences
Taylor [26]	1909	Diffraction	Photography	10^6	Yes
Dempster *et al.* [28]	1927	(i) Grating	Photography	10^5	Yes
		(ii) Fabry Perot	Photography	10^5	Yes
Janossy *et al.* [29]	1957	Michelson interferometer	Photomultiplier	10^5	Yes
Donstov *et al.* ([30])	1967	Fabry Perot	Image intensifier	10^3	No
Reynolds *et al.* [31]	1969	Fabry Perot	Image intensifier	10^2	Yes
Bozec *et al.* [32]	1969	Fabry Perot	Photography	10^2	Yes
Grishaev *et al.* [33]	1969	Jamin interferometer	Image intensifier	10^3	Yes
Ciamberlini *et al.* [27]	1994	Diffraction	Image intensifier and CCD	10^5	Yes

TABLE 10.2 Anticorrelation experiment with single-photon pulses from the radiative cascade. The last column corresponds to the expected number of coincidences for $\alpha = 1$. The measured coincidences show a clear anticorrelation effect. These data can be compared to Table 10.3

Trigger Rates	Singles Rates		Duration	Measured Coincidences	Expected Coincidences for $\alpha = 1$
$N_1(s^{-1})$	$N_R(s^{-1})$	$N_T(s^{-1})$	$\theta(s)$	$N_c\theta$	$\frac{N_R N_T}{N_1}\theta$
4720	2.45	3.23	1200	6	25.5
8870	4.55	5.75	17,200	9	50.8
1,21,00	6.21	8.44	14,800	23	64.1
20,400	12.6	17.0	19,200	86	204
36,500	31.0	40.6	13,200	273	456
50,300	47.6	61.9	8400	314	492
67,100	71.5	95.8	3600	291	367

allowed the adjustment of the gates with an accuracy of 0.1 ns. The system also yielded various time-delay spectra, useful for consistency checks.

Table 10.2 shows the measured counting rates for different values of the excitation rate of the cascade. The corresponding values of α have been plotted in Fig. 10.5 as a function of $N\tau_{\text{gate}}$. As expected, the violation of inequality (10.84) increases as $N\tau_{\text{gate}}$ decreases, but the signal decreases simultaneously, and it becomes necessary to accumulate the data for periods of time long enough to achieve a reasonable statistical accuracy. A maximum violation of more than 13 standard deviations has been obtained for a counting time of five hours (second line of Table 10.2). The value of α then is 0.18(6), corresponding to a total number of coincidences of 9, instead of the minimum value of 50 expected for a quasi-classical pulse.

10.3.4.2 Attenuated Classical Pulses

To confirm our arguments experimentally, and to test the photon-counting system, we also studied light from a pulsed light-emitting diode (LED). It produced light pulses with a rise time of 1.5 ns and a fall time about 6 ns. The gates, triggered by the electric pulses driving the photodiode, were 9 ns wide and had an almost complete overlap with the light pulses.

The source was attenuated to a level corresponding to one detection per 1,000 pulses emitted. With a detector quantum efficiency of about 10%, the average energy per pulse can be estimated to be about 0.01 photon. In the context of Table 10.1, this source certainly would have been considered a source of single photons. The results presented in Table 10.3 show that it is definitely not the

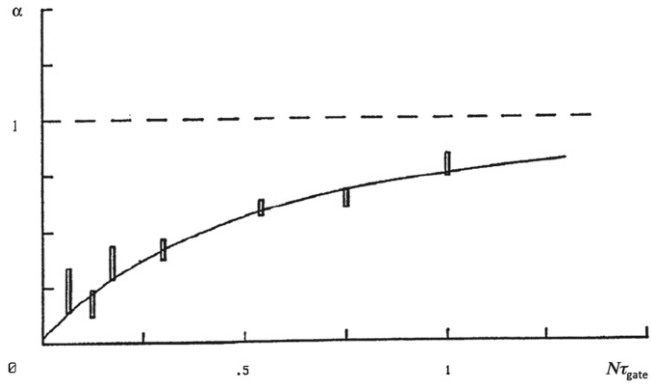

FIGURE 10.5 Correlation parameter α as a function of the excitation rate of the cascade N. The value of α smaller than 1 is the signature of an anticorrelation, corresponding to the one-photon behavior (no classical theory of light can predict a parameter α less than 1). The solid line is the prediction of quantum optics, taking into account the possibility that more than one atom is excited during one gate of duration τ_{gate}: For a single emitter, α would be zero.

TABLE 10.3 Anticorrelation experiment for light pulses from an attenuated photodiode (0.01 Photon/Pulse). The last column corresponds to the expected number of coincidences for $\alpha = 1$. All the measured coincidences are compatible with $\alpha = 1$; there is no evidence of anticorrelation. Note that the singles rates are similar to the ones of Table 10.2

Trigger rates	Singles rates		Duration	Measured coincidences	Expected coincidences for $\alpha = 1$
$N_1(s^{-1})$	$N_{2r}(s^{-1})$	$N_{2f}(s^{-1})$	$\theta(s)$	$N_c\theta$	$\frac{N_R N_T}{N_1}\theta$
4760	3.02	3.76	31200	82	74.5
8880	5.58	7.28	31200	153	143
12,130	7.90	10.2	25,200	157	167
20,400	14.1	20.0	25,200	341	349
35,750	26.4	33.1	12,800	329	313
50,800	44.3	48.6	18,800	840	798
67,600	69.6	72.5	12,800	925	955

case. The quantity α (of inequality (10.84)) is consistently found very close to 1; i.e., no anticorrelation is observed. In fact, the coincidence rate is exactly in agreement with the limit of inequality (10.84).

This experiment thus supports the claim that light emitted by an attenuated classical source does not exhibit one-photon behavior on a beamsplitter, even in

the case of very attenuated light pulses with an average energy by pulse much less than the energy of a photon.

10.3.4.3 Conclusion: Anticorrelation as a Characteristic Property of Single Photons

The experiments presented in this subsection confirm that anticorrelation on a beamsplitter is a very clear criterion for discriminating between a one-photon light pulse and a quasi-classical light pulse. A pulse produced by a classical source, even attenuated to a level of 10^{-2} average photon number per pulse, has the behavior expected for a quasi-classical pulse: one observes coincidences in agreement with the inequality (10.84). In contrast, we have been able to produce one-photon pulses for which the number of coincidences was so small that a violation of inequality (10.84) by more than 13 standard deviations was observed. This last result can also be considered as strong experimental evidence against semi-classical theories of light, which never predict a violation of inequality (10.84).

10.4 SINGLE-PHOTON INTERFERENCES

10.4.1 Wave-Particle Duality in Textbooks

Many introductory courses in Quantum Mechanics—whether or not they choose an historical perspective—begin with an "experiment" exhibiting the wave-particle duality of light and matter. This experiment is usually presented by showing an interference pattern, for instance in a Young's slit experiment. Such a phenomenon can be interpreted by invoking a wave that passes through both holes: it is well known that the resulting intensity then depends on the "path difference" Δ, and exhibits a modulation depending on the interference order $p = \Delta/\lambda$, where λ is the wavelength. On the other hand, the "particle" character is usually considered obvious for matter particles such as electrons, neutrons, or atoms, whereas it is actually not obvious for light, as discussed in the previous sections. In the latter case it is therefore useful, before looking for interferences, to present experimental proof that the source S emits well-separated single-photon pulses: if it were not the case, the discussion would be pointless. This is why we have addressed the question of single-photon interferences with the source described in 10.3.4.1.

10.4.2 Interferences with a Single Photon

The quantum theory of light predicts indeed that interferences will happen even with one-photon pulses (see for instance [17] for a detailed calculation). We have thus built a Mach-Zehnder interferometer, keeping the same source and the same beamsplitter as in Fig. 10.3, but removing the detectors on both sides of the beam splitter, and recombining the two beams on a second beam

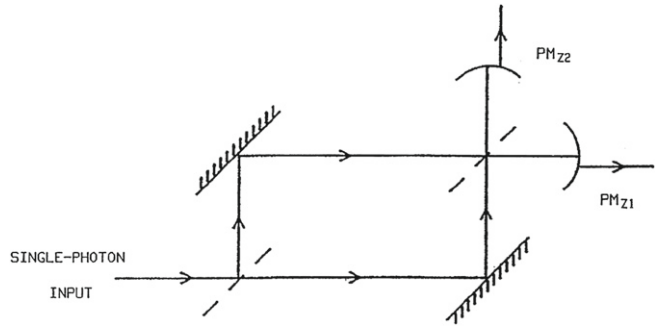

FIGURE 10.6 Single-photon interference experiment. The source and the beamsplitter are similar to Fig. 10.3, but are now configured as a Mach-Zehnder interferometer. The detectors are gated, as in Fig. 10.3, synchronously with the light pulses.

splitter (Fig. 10.6) [5]. The detection rates in the two outputs (1) and (2) are expected to be modulated as a function of the path difference in both arms of the interferometer. To guarantee that we are still working with one-photon pulses, the detectors $PM1$ and $PM2$ are gated synchronously with the pulses, as they were in the experiment of Section 10.3.4.1.

The interferometer has been carefully designed and built to give high-visibility fringes with the beam of large étendue (product of transverse area and solid angle) produced by our source (about 0.5 mm^2 rad^2). The reflecting mirrors and the beam splitters are $\lambda/50$ flat over a 40 mm diameter aperture. A mechanical system driven by piezoelectric transducers permits displacement of the mirrors while keeping their orientation exactly constant: this allows control of the path difference of the interferometer. Preliminary checks with classical light showed a strong modulation of the counting rates of PM_{Z1} and PM_{Z2} when the path difference is modified. For classical pulses shaped as the one-photon pulses from our source, the measured visibility was $V = 98.7(5)\%$, a value very close to the ideal value $V = 1$, showing the quality of the interferometer.

Figure 10.7 presents the results obtained by running this interferometer with the one-photon source. The numbers of counts during a given time interval are measured as a function of the path difference. In the first plots, the counting time at each position was 0.01 s, while it was 10 s for the last recordings. This run was performed with the sources in a regime corresponding to an anticorrelation parameter $\alpha = 0.2$, and therefore in the one-photon regime. These recordings clearly show the interference fringes building up "one-photon at a time." When enough data have been accumulated, the signal-to-noise ratio is high enough to allow a measurement of the visibility of the fringes. We repeated such measurements for various regimes of the source, corresponding to the different values of α shown in Fig. 10.5, and observed no deviation from the expected value $V = 98.7$, within the experimental noise, even in a regime where the source emits almost pure one-photon pulses. As predicted by the

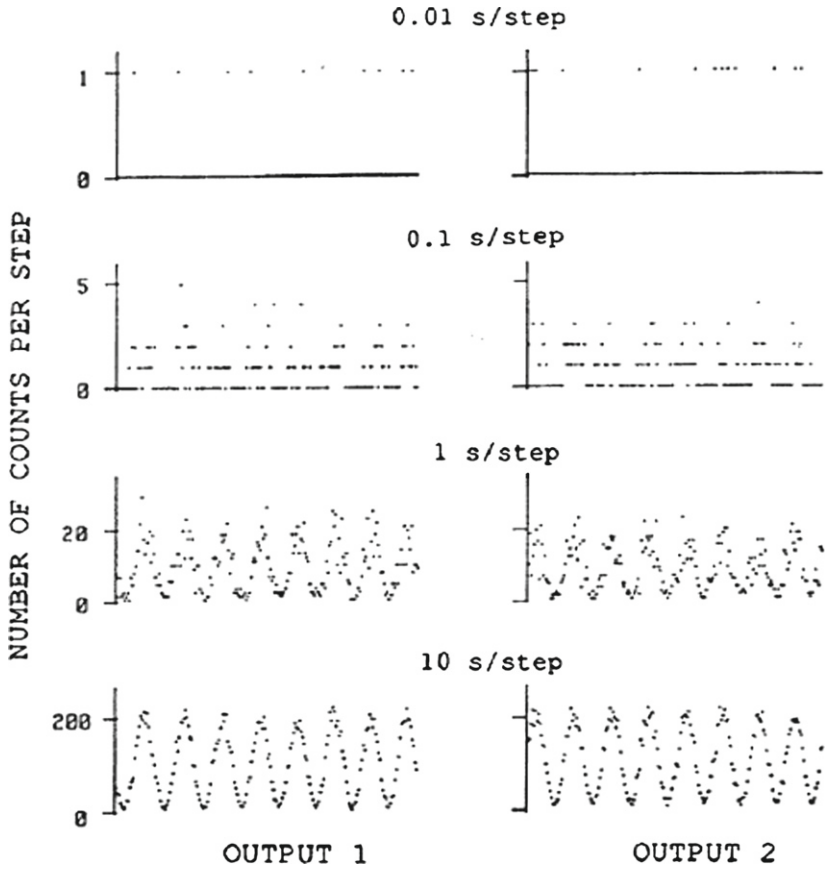

FIGURE 10.7 Number of detected counts in output (1) and (2) as a function of the path difference. The four sets of plots correspond to different counting times at each path difference. This experiment has been realized in the single-photon regime ($\alpha = 0.2$). Note that the interferograms of outputs (1) and (2) are complementary. Original plot for the experiment described in Ref. [5].

quantum theory of light, single-photon pulses do interfere. To our knowledge, this experiment (realized in 1985) was the first of this kind performed with a "fully quantum" light source, a source for which the anticorrelation effect was also directly observed [18].

10.5 FURTHER DEVELOPMENTS

10.5.1 Parametric Sources of Photon Pairs

During the same period as the experiments described above—between the early 1970s and the mid-1980s—another approach to generating photon pairs was

developed using parametric fluorescence from $\chi^{(2)}$ crystals, rather than atomic cascades [6,7]. In 1986, Hong & Mandel performed an experiment strongly related to the anticorrelation effect described above, though presented in a different way [8]. Since a full chapter in this book is devoted to such sources, here we only comment that the non-classical features of these photon pairs are similar to the ones described above, but with some notable differences:

- Due to phase-matching conditions, parametric photons are strongly correlated both in their emission times, with a time separation of the order of the inverse of the phase-matching bandwidth, and in their emission directions, due to the conservation of the photon momenta when "splitting" a pump photon into two parametric photons. As a consequence, the heralded photons can be collected with an efficiency orders of magnitude better than in an atomic cascade, and this has been intensively used in experiments.
- A parametric fluorescence experiment is significantly simpler and more reliable than an atomic cascade experiment. Indeed with such sources, a photon-anticorrelation experiment can now be a small and simple table-top experiment that can be done by students in lab work [43].

For these reasons, parametric fluorescence is now widely used to produce heralded single photons, and it is even possible to produce number states in well-defined spatio-temporal modes, and to reconstruct their Wigner functions using quantum homodyne tomography. This has been demonstrated both for one-photon [44] and two-photon Fock states [45]. It should be noted also that parametric photon pairs can be emitted from $\chi^{(3)}$ non-linear effects in optical fibers, rather than $\chi^{(2)}$ non-linear effects in crystals, as described in Chapter 13 of this book.

10.5.2 Other Heralded and "On-Demand" Single-Photon Sources

Many other types of single-photon sources have been proposed and implemented, using quantum dots, single molecules or atoms, possibly in the cavity QED regime, Nitrogen-vacancy centers in diamond, collectively enhanced quantum ensembles, all of which are described elsewhere in this book. Let us emphasize that some of these sources are getting close to being "on-demand" single-photon sources, meaning that the single photon is not only "heralded," but emitted in a "push-button" way at a prescribed time. This can be obtained rather easily from pulsed excitation of a single quantum emitter, but in addition it is desirable that the photon is emitted with a very high efficiency (that is, each "click" gives one and only one photon), and with a perfectly defined spatio-temporal mode (so that, for instance, high-quality quantum tomography of the single photon can be performed). A fully on-demand single-photon source is not yet available, but impressive progress has been achieved during the last 25 years.

10.5.3 "Delayed-Choice" Single-Photon Interference Experiments

To conclude, let us mention some recent developments in single-photon interferences. Following a famous proposal by Wheeler, a very convincing "delayed-choice" interference experiment has been performed by Jacques *et al.* using a Nitrogen-vacancy (NV) center in diamond as the single-photon source [20]. In this experiment, the "choice" of leaving the interferometer open—and thus observing the "which path" information—or closing the interferometer—and thus observing the interference fringes—is made while the photon is already inside a 50-m long interferometer. In even more recent experiments, it was shown that this choice can be made remotely, by using a second photon entangled with the photon inside the interferometer [21,22]. These experiments demonstrate the impressive control that can be obtained in manipulating single photons, offering more and more possibilities for applications in quantum information and quantum communications.

REFERENCES

[1] M.A. Nielsen and I.L. Chuang, "Quantum Computation and Quantum Information," Cambridge University Press (2010).
[2] S.J. Freedman and J.F. Clauser, "Experimental test of local hidden-variable theories," Phys. Rev. Lett. 28, pp. 938–941, 1972.
[3] J.F. Clauser, "Experimental Distinction Between Quantum and Classical Field-Theoretic Predictions for Photoelectric Effect," Phys. Rev. D 9, 853–860 (1974).
[4] A. Aspect, P. Grangier, and G. Roger, "Experimental Tests of Realistic Local Theories via Bell's Theorem," Phys. Rev. Lett. 47, 460–463 (1981).
[5] P. Grangier, G. Roger, and A. Aspect, "Experimental-Evidence for a Photon Anticorrelation Effect on a Beam Splitter—A New Light on Single-Photon Interferences," Europhys. Lett. 1, 173–179 (1986).
[6] D.C. Burnham and D.L. Weinberg, "Observation of Simultaneity in Parametric Production of Optical Photon Pairs," Phys. Rev. Lett. 25, 84–87 (1970).
[7] S. Friberg, C.K. Hong, and L. Mandel, "Measurement of Time Delays in the Parametric Production of Photon Pairs," Phys. Rev. Lett. 54, 2011–2013 (1985).
[8] C.K. Hong and L. Mandel, "Experimental Realization of a Localized One-Photon State," Phys. Rev. Lett. 56, 58–60 (1986).
[9] D.T. Pegg, R. Loudon, and P.L. Knight, "Correlations in Light Emitted by 3-Level Atoms," Phys. Rev. A 33, 4085–4091 (1986).
[10] B. Lounis and W. Moerner, "Single Photons on Demand from a Single Molecule at Room Temperature," Nature 407, 491–493 (2000).
[11] E.C.G. Sudarshan, "Equivalence of Semiclassical and Quantum Mechanical Descriptions of Statistical Light Beams," Phys. Rev. Lett. 10, 277–279 (1963).
[12] R.J. Glauber, "Coherent and Incoherent States of the Radiation Field," Phys. Rev. 131, 2766 (1963).
[13] H.J. Kimble, M. Dagenais, and L. Mandel, "Photon Anti-Bunching in Resonance Fluorescence," Phys. Rev. Lett. 39, 691–695 (1977).
[14] In his famous Lectures on Physics [46], Feynman cites Wave-Particle duality as the only mystery of quantum mechanics. However, two decades later [47], he emphasizes that up to that point he has missed to recognize the unique feature of entanglement.. and he immediately proposes to use it as a tool for quantum computing.
[15] R. Loudon, "The Quantum Theory of Light," Oxford University Press (2000).
[16] C. Gerry and P. Knight, "Introductory Quantum Optics," Cambridge University Press (2005).

[17] G. Grynberg, A. Aspect, and C. Fabre, "Introduction to Quantum Optics: From the Semi-Classical Approach to Quantized Light," Cambridge University Press (2010).
[18] A modern implementation of such an experiment illustrating wave-particle duality for a single-photon [48] has permitted our collaborators at ENS Cachan to produce a video showing directly the construction of an interference pattern photon by photon, with a single-photon source passing the single-photon test. This video can be found for instance at <http://www.lcf.institutoptique.fr/Alain-Aspect-homepage>.
[19] J.A. Wheeler, "Law Without Law," Princeton University Press (1984).
[20] V. Jacques, E. Wu, F. Grosshans, F. Treussart, P. Grangier, A. Aspect, and J.F. Roch, "Experimental Realization of Wheeler's Delayed-Choice Gedanken Experiment," Science 315, 966–968 (2007).
[21] F. Kaiser, T. Coudreau, P. Milman, D.B. Ostrowsky, and S. Tanzilli, "Entanglement-Enabled Delayed-Choice Experiment," Science 338, 637–640 (2012).
[22] A. Peruzzo, P. Shadbolt, N. Brunner, S. Popescu, and J.L. O'Brien, "A Quantum Delayed-Choice Experiment," Science 338, 634–637 (2012).
[23] A. Einstein, "Generation and Conversion of Light with Regard to a Heuristic Point of View," Annalen Der Physik 17, 132–148 (1905).
[24] Einstein's LichtQuanten was Named Photon Only Two Decades Later [49].
[25] A. Einstein, "On the Evolution of Our Vision on the Nature and Constitution of Radiation," Physikalische Zeitschrift 10, 817–826 (1909).
[26] G.I. Taylor, "Interference Fringes with Feeble Light," Proc. Cambridge Philos. Soc. 15, 114–115 (1910).
[27] C. Ciamberlini and G. Longobardi, "Real-Time Analysis of Diffraction Patterns, at Extremely Low-Light Levels," Opt. Lasers Eng. 21, 317–325 (1994).
[28] A.J. Dempster and H.F. Batho, "Light Quanta and Interference," Phys. Rev. 30, 644–648 (1927).
[29] L. Jánossy and Z. Náray, "The Interference Phenomena of Light at Very Low Intensities," Acta Phys. Hung. 7, 403–425 (1957).
[30] Y.P. Dontsov and A.I. Baz, "Interference Experiments with Statistically Independent Photons," Soviet Phys. JETP-Ussr 25, 1–5 (1967).
[31] G.T. Reynolds, S.K., and D.B. Scarl, "Interference Effects Produced by Single Photons," Nuovo Cimento Della Societa Italiana Di Fisica B-General Physics Relativity Astronomy And Mathematical Physics And Methods 61, 355–364 (1969).
[32] P. Bozec, M. Cagnet, and G. Roger, "Experiments on Interference in a Weak Light," Comptes Rendus Hebdomadaires Des Seances De L Academie Des Sciences Serie B 269, 883 (1969).
[33] I.A. Grishaev, N.N. Naugolny, L.V. Reprints, A.S. Tarasenk, and A.M. Shendero, "Interference Experiment and Photon Statistics for Synchrotron Radiation from Electrons in a Storage Ring," Soviet Phys. JETP-Ussr 32, 16 (1971).
[34] R. Glauber, Quantum Optics and Electronics, in Les Houches Summer School 1964, edited by C. DeWitt, Gordon and Breach, New York (1965).
[35] R.J. Glauber, "The Quantum Theory of Optical Coherence," Phys. Rev. 130, 2529 (1963).
[36] C. Cohen-Tannoudji, J. Dupont-Roc, and G. Grynberg, "Photons and Atoms-Introduction to Quantum Electrodynamics," Wiley-VCH (1997).
[37] L. Mandel and E. Wolf, "Optical Coherence and Quantum Optics," Cambridge University Press (1995).
[38] A.L. Schawlow and C.H. Townes, "Infrared and Optical Masers," Phys. Rev. 112, 1940 (1958).
[39] J. Goodman, "Statistical Optics," Vol. 1, New York, Wiley-Interscience, 567 p. (1985).
[40] This remark was used in the experiment where we observe an interference effect for a single-photon emitted jointly by two atoms flying in opposite directions after a molecular photodissociation [50]. The reason why this observation was successful is that the time of the dissociation, and thus of the leading-edge of the single-photon wave-packet, was precisely known, since the photodissociation was effected by a short laser pulse.
[41] C.K. Hong, Z.Y. Ou, and L. Mandel, "Measurement of Subpicosecond Time Intervals Between 2 Photons by Interference," Phys. Rev. Lett. 59, 2044–2046 (1987).
[42] This scheme is the one that was used in the experiment [5] presented in Section 10.3. A related scheme was proposed independently in [51].

[43] See for instance <http://www.institutoptique.fr/Formation/Ingenieur-Grande-Ecole/Travaux-Pratiques/Physique-quantique-atomique-nanophysique>at Institut d'Optique *Graduate School*.
[44] A.I. Lvovsky, H. Hansen, T. Aichele, O. Benson, J. Mlynek, and S. Schiller, "Quantum State Reconstruction of the Single-Photon Fock State," Phys. Rev. Lett. 87, 050402 (2001).
[45] A. Ourjoumtsev, R. Tualle-Brouri, and P. Grangier, "Quantum Homodyne Tomography of a Two-Photon Fock State," Phys. Rev. Lett. 96 (2006).
[46] R.P. Feynman, "Lectures on Physics," Addison-Wesley (1963).
[47] R.P. Feynman, "Simulating Physics with Computers," Int. J. Theor. Phys. 21, 467–488 (1982).
[48] V. Jacques, E. Wu, T. Toury, F. Treussart, A. Aspect, P. Grangier, and J.F. Roch, "Single-Photon Wavefront-Splitting Interference—An Illustration of the Light Quantum in Action," Eur. Phys. J. D 35, 561–565 (2005).
[49] G.N. Lewis, "The Conservation of Photons," Nature 118, 874–875 (1926).
[50] P. Grangier, A. Aspect, and J. Vigue, "Quantum Interference Effect for 2 Atoms Radiating a Single Photon," Phys. Rev. Lett. 54, 418–421 (1985).
[51] B. Saleh and M. Teich, "Sub-Poisson Light Generation by Selective Deletion from Cascaded Atomic Emissions," Opt. Commun. 52, 429–432 (1985).